



# Magnetofluorescent nanocomposites and quantum dots used for optimal application in magnetic fluorescence-linked immunoassay

H. Y. Tsai<sup>1,2</sup> · S. Y. Li<sup>3</sup> · C. Bor Fuh<sup>3</sup>

Received: 1 November 2017 / Revised: 7 December 2017 / Accepted: 4 January 2018 / Published online: 15 January 2018  
© Springer-Verlag GmbH Germany, part of Springer Nature 2018

## Abstract

Magnetofluorescent nanocomposites with optimal magnetic and fluorescent properties were prepared and characterized by combining magnetic nanoparticles (iron oxide@polymethyl methacrylate) with fluorescent nanoparticles (rhodamine 6G@mSiO<sub>2</sub>). Experimental parameters were optimized to produce nanocomposites with high magnetic susceptibility and fluorescence intensity. The detection of a model biomarker (alpha-fetoprotein) was used to demonstrate the feasibility of applying the magnetofluorescent nanocomposites combined with quantum dots and using magnetic fluorescence-linked immunoassay. The magnetofluorescent nanocomposites enable efficient mixing, fast re-concentration, and nanoparticle quantization for optimal reactions. Biofunctional quantum dots were used to confirm the alpha-fetoprotein (AFP) content in sandwich immunoassay after mixing and washing. The analysis time was only one third that required in ELISA. The detection limit was 0.2 pg mL<sup>-1</sup>, and the linear range was 0.68 pg mL<sup>-1</sup>–6.8 ng mL<sup>-1</sup>. This detection limit is lower, and the linear range is wider than those of ELISA and other methods. The measurements made using the proposed method differed by less than 13% from those obtained using ELISA for four AFP concentrations (0.03, 0.15, 0.75, and 3.75 ng mL<sup>-1</sup>). The proposed method has a considerable potential for biomarker detection in various analytical and biomedical applications.

**Keywords** Magnetofluorescent nanocomposites · Quantum dots · Magnetic fluorescence-linked immunoassay

## Introduction

Functional nanoparticles have been widely used in numerous analytical, biochemical, and material-related applications due to their special optical, electronic, magnetic, and chemical properties, but especially because of their quantum and size-dependent effects with various functional properties. Fluorescent and magnetic nanoparticles are particularly crucial functional nanoparticles due to their broad ranges of potential applications.

Fluorescent nanoparticles are widely used for imaging, sensing, and detection, with fluorescent dye-doped silica nanoparticles being one of the most valuable because they have high intensity, optical stability, and good biocompatibility. Magnetic nanoparticles are extensively employed for biomedical imaging and magnetic separation, with iron oxide nanoparticles being the most commonly used because of their biocompatibility [1–3]. Combining magnetic and fluorescent nanoparticles into magnetofluorescent nanocomposites (MFNs) with multifunctional properties would be favorable for biochemical applications such as biosensing, drug delivery, and clinical imaging [4–8].

The fluorescence intensity and/or magnetism of MFNs could be reduced by adjusting the experimental conditions during their synthesis and by involving the mutual reactions that occur when the two types of nanoparticles are combined [9]. Achieving high intensity and magnetism is challenging without optimization but is essential if MFNs are to be used in applications of separation, detection, and drug targeting. Biomarker detection is one of the main applications of MFNs due to its biomedical usefulness. Biomarker concentrations are typically low, and biomarkers are usually carried in a complex matrix [10]. Therefore, highly sensitive and selective

**Electronic supplementary material** The online version of this article (<https://doi.org/10.1007/s00216-018-0856-6>) contains supplementary material, which is available to authorized users.

✉ C. Bor Fuh  
cbfuh@ncnu.edu.tw

<sup>1</sup> School of Medical Applied Chemistry, Chung Shan Medical University, Taichung 402, Taiwan

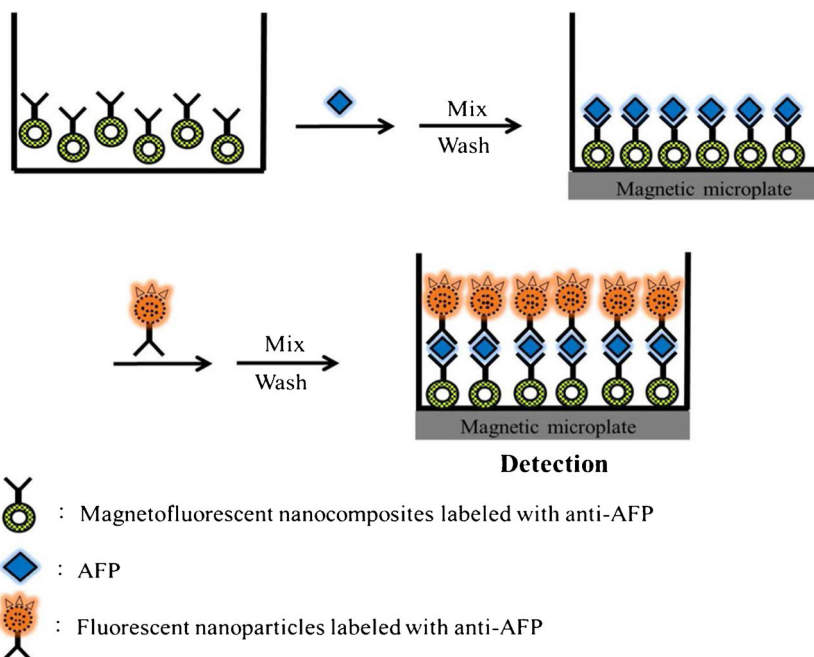
<sup>2</sup> Department of Medical Education, Chung Shan Medical University Hospital, Taichung 402, Taiwan

<sup>3</sup> Department of Applied Chemistry, National Chi Nan University, 1 University Road, Puli, Nantou 545, Taiwan

methods are essential in biomarker detection. Enzyme-linked immunosorbent assay (ELISA) is a reference method for biomarker detection and is routinely used for clinical diagnostics [11, 12]. However, it is laborious and time consuming; consequently, improvement of ELISA is necessary. Magnetic fluorescence-linked immunoassay using biofunctional nanoparticles has potential advantages over ELISA and deserves further investigation. The advantages of this method are that the analysis time can be reduced by two thirds, analyte mixing is more effective, nanocomposites can be optimized, and a lower detection limit can be achieved.

Figure 1 presents a schematic of magnetic fluorescence-linked immunoassay. MFNs labeled with anti-AFP ( $\alpha$ -fetoprotein) are placed in a microplate to capture AFP. The maximum number of MFNs that can be retained in the microplate and used in this method is determined by measuring their characteristic fluorescence intensity after a magnetic field has been applied to the bottom of the microplate. The loosely attracted nanocomposites are washed out of the microplate. AFP is added and mixed with the biofunctional nanocomposites, and then re-concentrated under a magnetic field after a washing step. Fluorescent nanoparticles labeled with anti-AFP are added to confirm the amount of AFP in sandwich immunoassay with characteristic fluorescence after the mixing and washing-out of unattracted nanoparticles. For this study, MFNs were prepared and characterized by combining magnetic nanoparticles (iron oxide@polymethyl methacrylate (PMMA)) with fluorescent nanoparticles (rhodamine 6G@mSiO<sub>2</sub>), which optimized both the magnetic and fluorescent properties of the MFNs. MFNs combined with quantum dots (QDs, fluorescent nanoparticles) were used to demonstrate AFP detection using magnetic fluorescence-linked immunoassay.

**Fig. 1** Schematic of magnetic fluorescence-linked immunoassay



## Material and methods

### Material

Ferrous chloride, ferric chloride, and cetyl trimethyl ammonium bromide were purchased from J.T. Baker (Phillipsburg, New Jersey, USA). Tetraethoxysilane, 3-aminopropyltriethoxysilane, diethylzinc, 1,6-hexamethylenediamine, methyl methacrylate (MMA), trioctylphosphine oxide, cadmium oxide, and phosphate-buffered saline (PBS) were purchased from Sigma-Aldrich (St. Louis, Missouri, USA). Rhodamine 6G (R6G), selenium, hexadecylamine, stearic acid, and bis(trimethylsilyl) sulfide were purchased from Acros (New Jersey, USA). Both AFP and anti-AFP were purchased from Abnova (Taoyuan, Taiwan). Polyvinyl alcohol and ammonium persulfate were purchased from Showa (Tokuyama, Japan). Sera were obtained from Jackson ImmunoResearch (West Grove, California, USA). Sera solutions were prepared by rehydration of freeze-dried solid with 10 mL of distilled water before use, as suggested by the supplier. Magnetic microplates were prepared by placing rare earth magnets under the microplate and used for re-concentration after mixing and washing steps. The magnetic field strength was  $2.5 \pm 0.1$  kG at the bottom of each microplate well.

### Preparation of functional nanoparticles

Iron oxide nanoparticles were prepared by chemically precipitating 0.1 g of ferrous chloride and 0.27 g of ferric chloride in a solution containing 50 mL of H<sub>2</sub>O and 4.5 mL of 28% (v/v) ammonium hydroxide. Iron oxide@PMMA nanoparticles were prepared by first adding 0.4 mL of 0.08 g mL<sup>-1</sup> iron

oxide, 0.25 mL of MMA, 1.39 mL of hexane, and 0.08 g of ammonium persulfate, in this sequence, to a mixture containing 0.5 mL of 0.5% polyvinyl alcohol and 0.012 g of sodium dodecylbenzenesulfone in 10 mL of H<sub>2</sub>O. The temperature of the above solution was then increased to and maintained at 80 °C for 5 h. The iron oxide@PMMA product was concentrated using magnet and washed with H<sub>2</sub>O three times.

The QDs used were composed of CdSe/ZnS with emission wavelength (590 nm) and were prepared as in our previous work [13]. In brief, solution A was prepared by mixing 0.0642 g of CdO, 4.83 g of TOPO, 2.41 g of hexadecylamine, and 0.569 g of stearic acid and by heating the mixture to 330 °C. Solution B (0.06 g of selenium in 2 mL of TOP) was added to solution A when solution A was cooled down to 250 °C. A 0.125 mL of solution C (0.1 mL of diethylzinc and 0.15 mL of bis(trimethylsilyl) sulfide) was then added to the mixture of solutions A and B and mixed completely. The newly formed quantum dots (CdSe/ZnS) were washed with methanol three times after removing the heat and cooling the quantum dots to room temperature. QD@mSiO<sub>2</sub> nanoparticles were prepared by first mixing 0.04 g of CdSe/ZnS in 25 mL of H<sub>2</sub>O containing 1 mL of chloroform and 0.115 g of cetyl trimethyl ammonium bromide, after which the solution was heated to and maintained at 60 °C for 15 min. Next, 0.1 mL of tetraethoxysilane, 2.4 mL of ethanol, and 1.75 mL of ammonium hydroxide were added and allowed to react for 3 h. The formed QD@mSiO<sub>2</sub> nanoparticles were concentrated and washed with ethanol five times. The excitation and emission wavelengths of the QD@mSiO<sub>2</sub> nanoparticles were 340 and 590 nm, respectively.

R6G@mSiO<sub>2</sub> nanoparticles were prepared first by mixing 0.025 g of R6G in 1 mL of ethanol with 0.11 g of cetyl trimethyl ammonium bromide in 25 mL of H<sub>2</sub>O in a flask, followed by heating at 60 °C in a water bath for 15 min. To the flask was then added 1.5 mL of tetraethoxysilane and 1 mL of ammonium hydroxide, and the mixture was allowed to react for 3 h. Subsequently, 1 mL of 3-aminopropyl-triethoxysilane was added, and the mixture was allowed to react for 2 h. The newly formed R6G@mSiO<sub>2</sub> nanoparticles were washed and centrifuged with ethanol three times and dried.

(Iron oxide@PMMA-R6G@mSiO<sub>2</sub>) nanocomposites were prepared in various ratios of the two constituents with fixing one constituent to determine the ratio that resulted in the optimal fluorescence intensity and magnetic susceptibility. The excitation and emission wavelengths of the MFNs were 500 and 550 nm, respectively. The optimal amount of R6G@mSiO<sub>2</sub> was obtained using the number ratios of fluorescent to magnetic nanoparticles of 1:85, 1:100, 1:125, and 1:170 with a fixed 7 mg of iron oxide@PMMA used. The optimal amount of iron oxide@PMMA was obtained using the number ratios of fluorescent to magnetic nanoparticles of 1:70, 1:100, 1:130, 1:160, and 1:190 with the R6G@mSiO<sub>2</sub> amount fixed according to the amount (25 mg) identified in the previous optimization.

To prepare [(iron oxide@PMMA)·(R6G@mSiO<sub>2</sub>)]@SiO<sub>2</sub>, different amounts of iron oxide@PMMA and R6G@mSiO<sub>2</sub> were mixed within a SiO<sub>2</sub> shell. Biofunctional MFNs and QD@mSiO<sub>2</sub> nanoparticles were prepared by coupling 1 mL of  $1.0 \times 10^{-7}$  M anti-AFP with 30 mg of amine-modified nanoparticles through the coupling reaction of *N*-hydroxysuccinimide and 1-ethyl-3-(3-dimethyl aminopropyl) carbodiimide in an ice bath for 2 h [2, 3, 14].

### Magnetic fluorescence-linked immunoassay

Figure 1 displays the reaction steps of the magnetic fluorescence-linked immunoassay. MFNs labeled with anti-AFP (biofunctional MFNs,  $5 \times 10^{11}$  in 150 μL of PBS solution) were placed in a microplate. A total of 100 μL of solution containing AFP, in concentrations of  $10^{-7}$ – $10^{-17}$  M, was mixed into each well, and the wells were washed twice using PBS solutions under a magnetic field for 5 min to remove the unreacted AFP. Fluorescent nanoparticles (QD@mSiO<sub>2</sub>) labeled with anti-AFP (biofunctional fluorescent probe,  $5 \times 10^{12}$  in 150 μL of PBS solution) were then added to react for 5 min and confirm the AFP in the AFP/anti-AFP complex. The fluorescence intensity in sandwich immunoassay using the biofunctional fluorescent probe was measured to determine the amount of AFP after the unreacted fluorescent probes were removed. A reference plot was established by plotting the percentages of the reacted fluorescent probe versus the various known concentrations of AFP added to the solution. The amount of AFP in samples was thus determined from the reference plot using the measured percentage of the reacted fluorescent probe.

## Results and discussion

### Characterization of functional nanoparticles and nanocomposites

The iron oxide, iron oxide@PMMA, and R6G@mSiO<sub>2</sub> nanoparticles had sizes of 5, 10, and 75 nm, respectively. Figure 2A, B presents TEM images of iron oxide@PMMA and R6G@mSiO<sub>2</sub>. The mesoporous morphology of mSiO<sub>2</sub> can be seen in Fig. 2B. The MFNs were prepared by directly coupling iron oxide@PMMA with R6G@mSiO<sub>2</sub>—producing [(iron oxide@PMMA-R6G@mSiO<sub>2</sub>)]—and by silica-wrapping iron oxide@PMMA with R6G@mSiO<sub>2</sub>—producing [(iron oxide@PMMA)·(R6G@mSiO<sub>2</sub>)]@SiO<sub>2</sub>. The objective of the MFN optimization was to maintain high magnetic susceptibility and fluorescence intensity while limiting the size of the MFNs to less than 100 nm. The MFNs produced through direct coupling were prepared using various ratios of iron oxide@PMMA to R6G@mSiO<sub>2</sub>, and the ratio that resulted in optimal magnetic susceptibility and



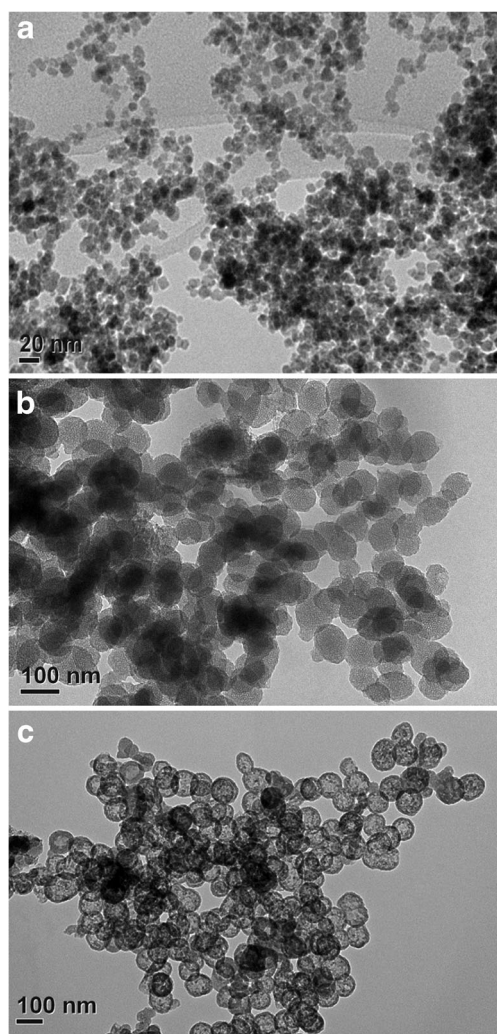


**Fig. 2** TEM images of **A** iron oxide@PMMA nanoparticles, **B** R6G@mSiO<sub>2</sub> nanoparticles, and **C** iron oxide@PMMA-R6G@mSiO<sub>2</sub> nanocomposites

fluorescence intensity was identified. The optimal amount of R6G@mSiO<sub>2</sub> was determined to be 25 mg, equivalent to an optimal number ratio of fluorescent to magnetic nanoparticles of 1:100 for a fixed amount of iron oxide@PMMA. The optimal amount of iron oxide@PMMA was determined to be 9 mg, equivalent to an optimal number ratio of fluorescent to magnetic nanoparticles of 1:130 for the fixed optimal amount of R6G@mSiO<sub>2</sub>. Figure S1A in the Electronic supplementary material (ESM) shows the absorption spectra of

MFNs and its precursors. There is a small difference in the spectra for three samples.

Table 1 presents a comparison of several MFN samples with sizes of approximately 85 nm. The size of iron oxide@PMMA nanoparticles was approximately 10 nm. The magnetic and fluorescent nanocomposites composed of iron oxide@PMMA and R6G@mSiO<sub>2</sub> had higher fluorescence intensity but lower magnetic susceptibility than those composed of iron oxide@PMMA and QD@mSiO<sub>2</sub> with a core/shell preparation. The MFNs prepared using direct coupling had higher fluorescence intensity and magnetic susceptibility than those obtained through core/shell preparation, potentially because direct coupling provided less shielding. Figure 2C displays a TEM image of the MFNs prepared using direct coupling. The size of the MFNs was 85 nm. The iron oxide@PMMA nanoparticles cannot be seen clearly due to the relative sizes of iron oxide@PMMA (10 nm) to R6G@mSiO<sub>2</sub> (75 nm) in MFNs of Fig. 2C. They are shown on the surface edge of some MFNs. MFN formation was verified from the infrared spectra of the MFNs and their precursors, and the spectra are presented in Fig. 3A. The formation of MFNs can be verified from their infrared spectra containing functional groups (< 1400 cm<sup>-1</sup> region) of R6G@mSiO<sub>2</sub> and functional groups (> 1400 cm<sup>-1</sup> region) of iron oxide@PMMA. The functional groups (468, 800, and 1100 cm<sup>-1</sup>) of SiO<sub>2</sub> from R6G@mSiO<sub>2</sub> can be seen in MFNs in Fig. 3A. The functional group (1720 cm<sup>-1</sup> (C=O); clearly seen and 590 cm<sup>-1</sup> (Fe-O); relatively weak) of iron oxide@PMMA can also be found in MFNs. Figure 3B illustrates the change in magnetic susceptibility of the MFNs and their precursors. The magnetic susceptibility decreases as surface modifications of iron oxide and iron oxide@PMMA proceed in Fig. 3B. The susceptibility of the MFNs was 27 emu g<sup>-1</sup>, several times higher than that reported in the literature [15–17]. High magnetic susceptibility would favor the application of magnetic force and the efficiency of this technique. MFNs prepared using direct coupling with an optimal ratio of fluorescent to magnetic nanoparticles (1:130) were used for all subsequent experiments.

### Magnetic fluorescence-linked immunoassay

The maximum number of MFNs labeled with anti-AFP (biofunctional MFNs) that were retained and used in the

**Table 1** Comparison of several magnetofluorescent nanocomposites

Magnetofluorescent nanocomposites	Fluorescent intensity (4 mg mL <sup>-1</sup> )	Magnetic susceptibility (emu g <sup>-1</sup> )
[(Iron oxide@PMMA)-(QD <sub>0</sub> @mSiO <sub>2</sub> )]@SiO <sub>2</sub>	35	20
[(Iron oxide@PMMA)-(QD <sub>g</sub> @mSiO <sub>2</sub> )]@SiO <sub>2</sub>	210	20
[(Iron oxide@PMMA)-(R6G@mSiO <sub>2</sub> )]@SiO <sub>2</sub>	5000	14
(Iron oxide@PMMA)-(R6G@mSiO <sub>2</sub> )	9000	27

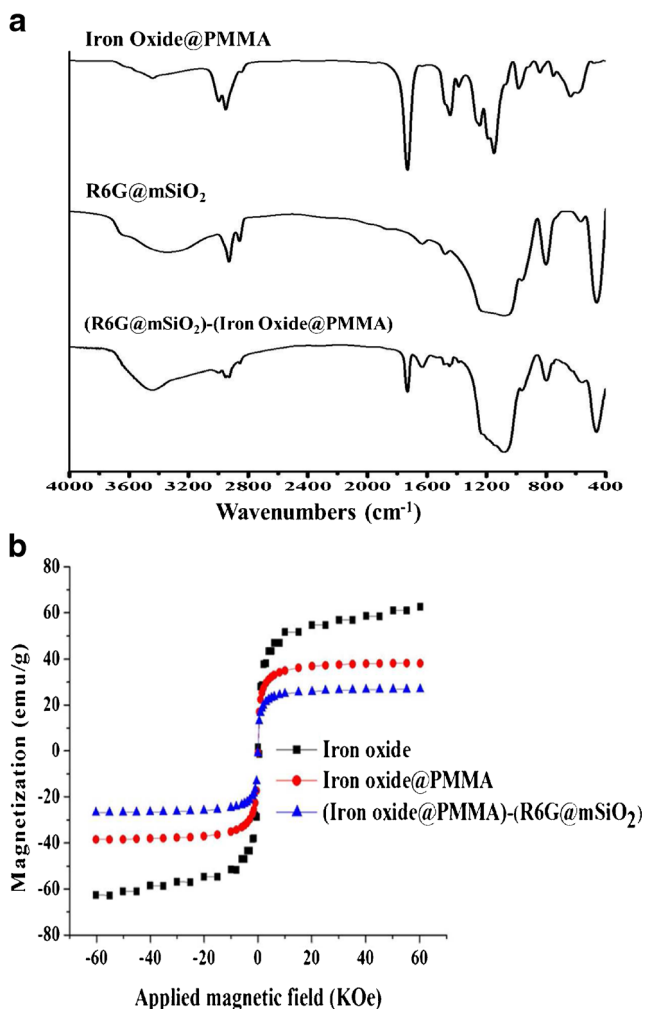
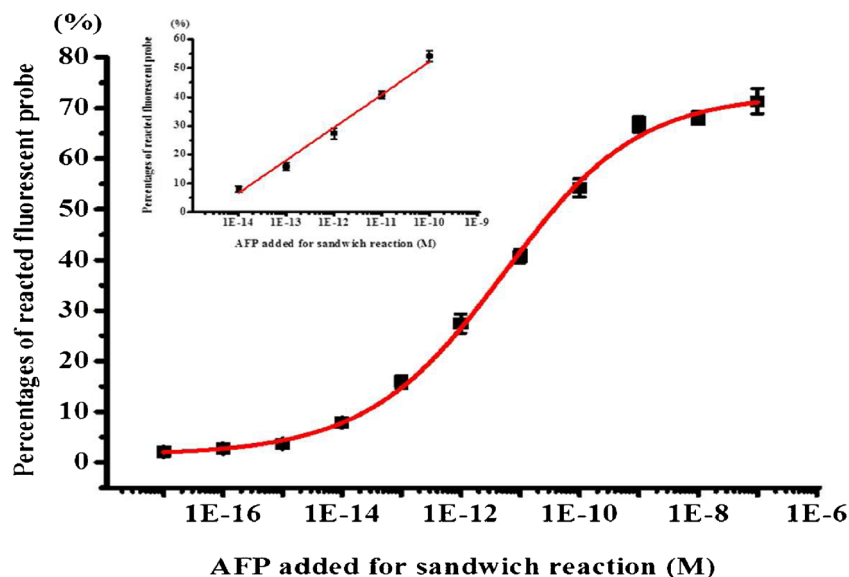


**Fig. 3** A Infrared spectra and B magnetic susceptibility of manetofluorescent nanocomposites and precursors

**Fig. 4** Reference plot of magnetic fluorescence-linked immunoassay



microplate sandwich reaction was determined to be  $5.0 \times 10^{11}$  by applying a magnetic force and measuring the resultant fluorescence. Fluorescence quantitation of MFNs is superior to weight quantization of magnetic nanoparticles for nanomaterials. The size of the QD@mSiO<sub>2</sub> nanoparticles was 45 nm. The optimal number of QD@mSiO<sub>2</sub> nanoparticles was  $5.0 \times 10^{12}$ , as determined by their fluorescence saturation in the sandwich reaction. The numbers of anti-AFP on each MFN and QD@mSiO<sub>2</sub> nanoparticle were determined to be 10 and 2, respectively, as calculated from the difference in the anti-AFP before and after labeling and using absorption measurements. Figure S1B (see ESM) shows the absorption spectra of MFNs-QD@mSiO<sub>2</sub> sandwich and its precursors. Figure S2 (see ESM) shows the TEM micrograph of MFNs-QD@mSiO<sub>2</sub> sandwich product with circling MFNs in green color and circling QD@mSiO<sub>2</sub> in orange color for several pairs. The proposed method has several advantages over ELISA. First, the interaction between antigen and antibody is more effective because of the large surface-to-volume ratio of nanoparticles. Second, all reactions occurred under nearly homogeneous conditions. Third, MFNs can be optimized. Finally, magnetic forces are useful for separation and re-concentration. Therefore, the total analysis time (28 min) for the proposed method is one thirds of that required for ELISA. A lower detection limit and wider linear range can be achieved.

Figure 4 presents an AFP reference plot determined using sandwich immunoassay for serum solutions with various added AFP concentrations. The relative standard deviation of each point in the figure was smaller than 5%. Figure S3 in the ESM shows the fluorescence spectra of MFNs,

**Table 2** Comparison of detection limit and linear range for AFP detection

Literature	Detection limit (ng mL <sup>-1</sup> )	Linear range (ng mL <sup>-1</sup> )	Ref
Anal. Chim. Acta 2011, 686, 115–120	2.5	5–70	[18]
Biosens. Bioelectron. 2014, 61, 245–250	0.005	0.01–12	[19]
Analyst 2012, 137, 393–399	0.05	0.1–50	[20]
Anal. Chem. 2015, 87, 2959–2965	0.0016	0.005–1.0	[21]
This study	0.0002	0.00068–6.8	

QDo@mSiO<sub>2</sub>, and MFNs-QDo@mSiO<sub>2</sub> sandwich samples. The excitation and emission wavelengths of MFNs were 500 and 550 nm. The excitation and emission wavelengths of QDo@mSiO<sub>2</sub> were 340 and 590 nm. The excitation and emission wavelengths of MFNs-QDo@mSiO<sub>2</sub> sandwich were 340 and 581 nm. In controlled selective studies, free AFP was replaced with a blank, free IgG, and free CEA at concentrations 10<sup>-11</sup>, 10<sup>-12</sup>, and 10<sup>-13</sup> M. The percentages of the reacted fluorescent probe were all less than 7% and did not affect the reference plot, indicating the favorable selectivity of this method. The linear range is 10<sup>-14</sup> M (0.68 pg mL<sup>-1</sup>) to 10<sup>-10</sup> M (6.8 ng mL<sup>-1</sup>), and the detection limit is 0.2 pg mL<sup>-1</sup> based on a signal-to-noise ratio of 3.0. The linear range is substantially wider than those for ELISA and other methods [18–21], and the detection limit is also substantially lower [18–21]. Table 2 provides a comparison between the detection limit and linear range of the current AFP detection method and those reported in the literature.

ELISA is one of the most widely used methods for detecting AFP. To compare the proposed method with ELISA, serum samples spiked with four AFP concentrations (0.03, 0.15, 0.75, and 3.75 ng mL<sup>-1</sup>) were tested. The AFP values measured using the proposed method and ELISA were 0.034, 0.14, 0.71, and 3.56 ng mL<sup>-1</sup> and 0.036, 0.13, 0.80, and 3.84 ng mL<sup>-1</sup>, respectively. The measurements made using the proposed method differed to the spiked values from 5.1 to 13.3%, with a mean of 7.6%, whereas the measurements made using the proposed method differed from those made using ELISA from 5.8 to 12.6%, with a mean of 8.3%.

## Conclusions

The experimental results demonstrated that MFNs with high magnetic susceptibility and fluorescence intensity were prepared and optimized. MFNs combined with fluorescent QDs were employed for biomarker detection using the magnetic fluorescence-linked immunoassay. The proposed method has a lower detection limit and wider linear range than ELISA and other biomarker detection methods. The proposed method has considerable potential for various analytical and biomedical applications.

**Acknowledgments** We thank Mr. S. S. Chuang, Mr. Lokesh Bettad, and Ms. Y. S. Lu for technical assistance.

**Funding information** This work was supported by the Ministry of Science and Technology in Taiwan (Grant MOST-104-2119-M-260-003).

## Compliance with ethical standards

**Conflict of interest** The authors declare that they have no conflict of interest.

## References

- Reddy LH, Arias JL, Nicolas J, Couvreur P. Magnetic nanoparticles: design and characterization, toxicity and biocompatibility, pharmaceutical and biomedical applications. *Chem Rev.* 2012;112:5818–78.
- Tsai HY, Chan JR, Li YC, Cheng FC, Fuh CB. Determination of hepatitis B surface antigen using magnetic immunoassays in a thin channel. *Biosens Bioelectron.* 2010;25:2701–5.
- Tsai HY, Hsieh YC, Chan JR, Su YM, Chang YC, Fuh CB. Effects of particle characteristics on magnetic immunoassay in a thin channel. *Biosens Bioelectron.* 2011;28:38–43.
- Qiu Z, Shu J, He Y, Lin Z, Zhang K, Lv S, et al. CdTe/CdSe quantumdot-based fluorescent aptasensor with hemin/G-quadruplex DNzyme for sensitive detection of lysozyme using rolling circle amplification and strand hybridization. *Biosens Bioelectron.* 2017;87:18–24.
- Lin Y, Zhou Q, Tang D, Niessner R, Knopp D. Signal-on photoelectrochemical immunoassay for aflatoxin B<sub>1</sub> based on enzymatic product-etching MnO<sub>2</sub> nanosheets for dissociation of carbon dots. *Anal Chem.* 2017;89:5637–45.
- Qiu Z, Shu J, Tang D. Bioresponsive release system for visual fluorescence detection of carcinoembryonic antigen from mesoporous silica nanocontainers mediated optical color on quantum dot-enzyme-impregnated paper. *Anal Chem.* 2017;89:5152–60.
- Wang G, Zhang X, Liu Y, Hu Z, Mei X, Uvda K. Magneto-fluorescent nanoparticles with high intensity NIR emission, T<sub>1</sub>- and T<sub>2</sub>-weighted MR for multimodal specific tumor imaging. *J Mater Chem B.* 2015;3:3072–80.
- Chen M, He Y, Chen X, Wang J. Quantum dots conjugated with Fe<sub>3</sub>O<sub>4</sub>-filled carbon nanotubes for cancer-targeted maging and magnetically guided drug delivery. *Langmuir.* 2012;28:16469–76.
- Sathe R, Agrawal A, Nie S. Mesoporous silica beads embedded with semiconductor quantum dots and iron oxide nanocrystals: dual-function microcarriers for optical encoding and magnetic separation. *Anal Chem.* 2006;78:5627–32.
- Wu J, Fu Z, Yan F, Ju H. Biomedical and clinical applications of immunoassays and immunosensors for tumor markers. *Trends Anal Chem.* 2007;26:679–88.

11. Boonham N, Kreuze J, Winter S, van der Vlugt R, Bergervoet J, Tomlinson J, et al. Methods in virus diagnostics: from ELISA to next generation sequencing. *Virus Res.* 2014;186:20–31.
12. Lequin RM. Enzyme immunoassay (EIA)/enzyme-linked immunosorbent assay (ELISA). *Clin Chem.* 2005;51:2415–8.
13. Tsai HY, Chuang MJ, Chou BC, Yang SF, Fuh CB. Quantitative improvement of magnetic immunoassays in thin channels using magnetofluorescent nanocomposites. *Sensors Actuators B Chem.* 2016;223:834–8.
14. Tang D, Su B, Tang J, Ren J, Chen G. Nanoparticle-based sandwich electrochemical immunoassay for carbohydrate antigen 125 with signal enhancement using enzyme-coated nanometer-sized enzyme-doped silica beads. *Anal Chem.* 2010;82:1527–34.
15. Gao J, Zhang W, Huang P, Zhang B, Zhang X, Xu B. Intracellular spatial control of fluorescent magnetic nanoparticles. *J Am Chem Soc.* 2008;130:3710–1.
16. Wang F, Chen X, Zhao Z, Tang S, Huang X, Lin C, et al. Synthesis of magnetic, fluorescent and mesoporous core-shell-structured nanoparticles for imaging, targeting and photodynamic therapy. *J Mater Chem.* 2011;21:11244–52.
17. Yi DK, Selvan ST, Lee SS, Papaefthymiou GC, Kunolaliya D, Ying JY. Silica-coated nanocomposites of magnetic nanoparticles and quantum dots. *J Am Chem Soc.* 2005;127:4990–1.
18. Huang X, Ren J. Gold nanoparticles based chemiluminescent resonance energy transfer for immunoassay of alpha fetoprotein cancer marker. *Anal Chim Acta.* 2011;686:115–20.
19. Qi T, Liao J, Li Y, Peng J, Li W, Chu B, et al. Label-free alpha fetoprotein immunosensor established by the facile synthesis of a palladium-graphene nanocomposite. *Biosens Bioelectron.* 2014;61:245–50.
20. Qi H, Ling C, Ma Q, Gao Q, Zhang C. Sensitive electrochemical immunosensor array for the simultaneous detection of multiple tumor markers. *Analyst.* 2012;137:393–9.
21. Zhang J, Wang S, Liu K, Wei Y, Wang X, Duan Y. Novel signal-enhancing immunoassay for ultrasensitive biomarker detection based on laser-induced fluorescence. *Anal Chem.* 2015;87:2959–65.